Editors' Suggestion   Featured in Physics

Rare ^{40}K Decay with Implications for Fundamental Physics and Geochronology

M. Stukel,[1] L. Hariasz,[1] P. C. F. Di Stefano,[1,*] B. C. Rasco,[2] K. P. Rykaczewski,[2] N. T. Brewer,[2,3] D. W. Stracener,[2]
Y. Liu,[2] Z. Gai,[4] C. Rouleau,[4] J. Carter,[5] J. Kostensalo,[6] J. Suhonen,[7] H. Davis,[8,9] E. D. Lukosi,[8,9] K. C. Goetz,[10]
R. K. Grzywacz,[2,3,11] M. Mancuso,[12] F. Petricca,[12] A. Fijałkowska,[13] M. Wolińska-Cichocka,[2,3,14] J. Ninkovic,[15]
P. Lechner,[15] R. B. Ickert,[16] L. E. Morgan,[17] P. R. Renne,[5,18] and I. Yavin[†]

(KDK Collaboration)

[1]*Department of Physics, Engineering Physics & Astronomy, Queen's University, Kingston, Ontario K7L 3N6, Canada*
[2]*Physics Division, Oak Ridge National Laboratory, Oak Ridge, Tennessee 37831, USA*
[3]*Joint Institute for Nuclear Physics and Application, Oak Ridge National Laboratory, Oak Ridge, Tennessee 37831, USA*
[4]*Center for Nanophase Materials Sciences, Oak Ridge National Laboratory, Oak Ridge, Tennessee 37831, USA*
[5]*Berkeley Geochronology Center, Berkeley, California 94709, USA*
[6]*Natural Resources Institute Finland, Joensuu FI-80100, Finland*
[7]*Department of Physics, University of Jyväskylä, Jyväskylä FI-40014, Finland*
[8]*Department of Nuclear Engineering, University of Tennessee, Knoxville, Tennessee 37996, USA*
[9]*Joint Institute for Advanced Materials, University of Tennessee, Knoxville, Tennessee 37996, USA*
[10]*Nuclear and Extreme Environments Measurement Group, Oak Ridge National Laboratory, Oak Ridge, Tennessee 37831, USA*
[11]*Department of Physics and Astronomy, University of Tennessee, Knoxville, Tennessee 37996, USA*
[12]*Max-Planck-Institut für Physik, Munich D-80805, Germany*
[13]*Faculty of Physics, University of Warsaw, Warsaw PL-02-093, Poland*
[14]*Heavy Ion Laboratory, University of Warsaw, Warsaw PL-02-093, Poland*
[15]*MPG Semiconductor Laboratory, Munich D-80805, Germany*
[16]*Department of Earth, Atmospheric, and Planetary Sciences, Purdue University, West Lafayette, Illinois 47907, USA*
[17]*U.S. Geological Survey, Geology, Geophysics, and Geochemistry Science Center, Denver, Colorado 80225, USA*
[18]*Department of Earth and Planetary Science, University of California, Berkeley, California 94720, USA*

Potassium-40 is a widespread, naturally occurring isotope whose radioactivity impacts subatomic rare-event searches, nuclear structure theory, and estimated geological ages. A predicted electron-capture decay directly to the ground state of argon-40 has never been observed. The KDK (potassium decay) collaboration reports strong evidence of this rare decay mode. A blinded analysis reveals a nonzero ratio of intensities of ground-state electron-captures (I_{EC^0}) over excited-state ones (I_{EC^*}) of $I_{\mathrm{EC}^0}/I_{\mathrm{EC}^*} = 0.0095 \overset{\mathrm{stat}}{\pm} 0.0022 \overset{\mathrm{sys}}{\pm} 0.0010$ (68% C.L.), with the null hypothesis rejected at 4σ. In terms of branching ratio, this signal yields $I_{\mathrm{EC}^0} = 0.098\% \overset{\mathrm{stat}}{\pm} 0.023\% \overset{\mathrm{sys}}{\pm} 0.010\%$, roughly half of the commonly used prediction, with consequences for various fields [L. Hariasz *et al.*, companion paper, Phys. Rev. C **108**, 014327 (2023)].

Potassium-40 (^{40}K) is a long-lived radioactive isotope figuring prominently in a variety of fields from geology to searches for exotic subatomic particles and processes. ^{40}K is one of the three naturally occurring K isotopes. It is fairly common, representing about a ten-thousandth of natural potassium, and contributing roughly half of the radioactivity in the human body. It plays an important role in geochronology, through K/Ar and ^{40}Ar/^{39}Ar dating. In addition, its commonness makes ^{40}K a challenging background in many particle-physics experiments looking for rare processes, such as dark matter interactions or

neutrinoless double-beta decay ($0\nu\beta\beta$). Lastly, its decay scheme involving all three types of beta decay is rare, and impactful to nuclear-structure analyses [1]. Surprisingly, among those decays, the electron-capture (EC) transitions of ^{40}K to ^{40}Ar are incompletely known.

From the standpoint of particle physics exploring the fundamental nature of our Universe, a host of experiments are looking for putative dark-matter particles that could make up the bulk of matter [2]. Low-energy x rays and Auger electrons emitted after ^{40}K electron capture fall in the signal region expected in many dark-matter models; as
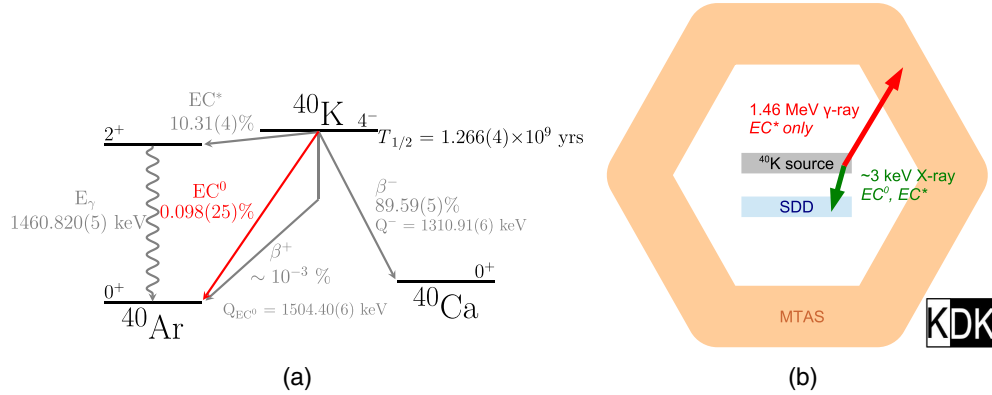
FIG. 1.   (a) Decay scheme of ^{40}K. The branching ratios and half-life were calculated from our determination of I_{EC^0}/I_{EC^*} and from literature values for T^- (partial half-life of the β^- decay) and T^* (partial half-life of EC*) [23]. The γ transition energy is taken from [22], Q_{EC^0} and Q^- are taken from [24]. (b) Schematic of how the KDK experiment distinguishes EC* from EC^0 (not to scale).

such, electron capture is a significant background in many experiments of this type. In the case of decays to an excited stated of ^{40}Ar (EC*), the high-energy γ ray emitted during deexcitation provides a means of identifying and rejecting the problematic x ray; however, in the case of electron-capture decay to ground state (EC^0), there is no such means to tag this background. Because of the chemical similarity between Na and K, trace amounts of this ^{40}K are always present even in ultraradiopure NaI scintillating crystals used for dark matter detection [3–6]. The DAMA/LIBRA experiment employs such a detector and has claimed an observation of a signal consistent with particle dark matter for over 20 years [7]. However, it has been noted that the lack of an experimental verification of the ground state electron capture of ^{40}K can pose a challenge to any interpretation of the DAMA/LIBRA results in terms of a dark matter model [8].

With a total half-life of over a billion years, ^{40}K is one of the longest-lived naturally occurring radioactive isotopes on Earth, motivating its long-standing use as a dating tool in geology and archaeology. Moreover, measuring samples with various techniques provides insight into the thermal history of the Earth, and variation in K/Ar and ^{40}Ar/^{39}Ar ages can significantly affect our understanding of terrestrial and solar-system evolution. Advances in the analytical precision of the K/Ar [9] and ^{40}Ar/^{39}Ar [10] techniques have caused the field to address systematic uncertainties, including those in the total and electron-capture decay rates. Though there have long been calls for the EC^0 contribution to be determined [11,12], many commonly used reviews in the field ignore it [13,14]. However, it has recently been pointed out that this omission could lead to an overestimation of a sample age by tens of millions of years [15].

The overall ^{40}K decay scheme, including the measurement of this Letter, is displayed in Fig. 1(a). The principal disintegration mode is by β^- to ^{40}Ca. It dominates electron capture, which is mainly to an excited state of ^{40}Ar, with a

rarer, and previously unobserved, decay to the ground state which is the focus of this Letter. There is also a much weaker decay by positron emission to ^{40}Ar. With our Letter, the ground-state electron capture of ^{40}K is the only observed third-forbidden unique electron-capture decay [16]. For such a transition the theories are challenging to validate [17,18] leading to a wide spread of reported intensity values, $I_{EC^0} = (0.0$–$0.8)\%$ for the assumed or predicted branching ratio [8,13,15,19–22]. In a regime which is difficult to access theoretically, the KDK (potassium decay) measurement informs the extent of suppression of $0\nu\beta\beta$ processes probing physics beyond the standard model [1].

The focus of this Letter is the first measurement of the electron-capture decay to ground state, carried out by the KDK Collaboration [25]. This experiment is challenging due to the high forbiddenness of the direct ground-state electron capture and the dominating, much more frequent excited-state electron capture, necessitating exceptionally strong background rejection. Experiments wishing to make this measurement must be able to distinguish between excited- and ground-state electron-capture events with exceptionally high precision. In KDK, this is achieved by combining a very sensitive detector to trigger on x rays from both forms of electron capture occurring in a ^{40}K source, with a high efficiency tagger to identify the γ rays from EC*, and thus distinguish both types of decays [Fig. 1(b)]. This enables us to determine the ratio of their intensities, $\rho = I_{EC^0}/I_{EC^*}$.

The discrimination between excited and ground-state events was achieved through a unique detector configuration ([26] and Fig. 2 of [27]). When an electron capture occurs in the source, a high-resolution, low-energy threshold x-ray detector is available to observe the associated $\sim$3 keV characteristic x ray. Following such a trigger in the inner detector, a coincidence window is opened with a large, outer, γ-ray tagger which completely surrounds the source and inner detector. If the decay is to the excited state, the tagger should identify the accompanying γ ray. In practice, various efficiencies and backgrounds affect this

scheme, and events are referred to either as coincident or anticoincident. As described further on, our analysis untangles how many are actually EC^0 decays as opposed to EC^* decays.

The inner detector is a 100 mm^2 active surface area silicon drift detector [28] (SDD). The detector is contained inside the γ-ray tagger, the modular total absorption spectrometer (MTAS) from Oak Ridge National Laboratory [29]. MTAS is a metric tonne array of NaI(Tl) scintillators surrounding the inner detector. The tagging efficiency for 1.46 MeV γ rays is $\sim 98\%$. Details of the setup, including the energy calibration, can be found in our technical publication [26].

The ^{40}K source was made from enriched KCl [16.1(6)% ^{40}K abundance in K] thermally deposited over 1 cm diameter onto a graphite substrate. The $\sim 9 \times 10^{17}$ atoms of ^{40}K in the source have an activity of ~ 16 Bq, equivalent to that found in two medium-sized bananas [30], and the source is 5.1(9) μm thin to allow the x rays to escape from it. The source rests directly in front of the SDD and is centered inside MTAS.

Data presented in what follows represent our full 34 live-day dataset opened in January 2022. To avoid biases during the analysis, the anti-coincident SDD spectrum was blinded over the electron capture signal region and the silicon escape peak region while cuts and analysis methods were established. To help understand backgrounds, data were analyzed at 3 coincidence windows (1, 2, and 4 μs), with the middle one chosen in advance for the main result. Low-level data analysis is described elsewhere [26,27].

To determine the ratio of intensities between the ground and excited-state electron captures, our analysis compares the number of coincident and anticoincident Ar x rays. In order to achieve this we need to understand the respective SDD spectra in Fig. 2. In the energy region of interest, they each contain a continuum and several x-ray lines, all dominated by the source and its related interactions.

Thanks to the exceptional resolution of the SDD [26], the elemental x-ray lines, each modeled with a Gaussian, are easily identifiable. The shape for each element is the same in both the coincident and anticoincident spectra, though the intensities differ. The Ar x-ray lines at ~ 3 keV from electron capture are the focus of this Letter; the coincident spectrum unambiguously provides the position and shape of the sought-after anticoincident line. The relative coincident and anticoincident intensities of this contribution depend on the branching ratios, known x-ray emission probabilities of EC^0 and EC^* branches [31], and, additionally, on experimental effects that are (i) the MTAS tagging efficiency, (ii) the possibility of spurious coincidences with the MTAS background, and (iii) the possibility of γ interactions with the SDD.

At energies of a few keV, the continuous spectral elements are modeled with exponential and flat components. The prime contributor to these events are the ^{40}K β^-,
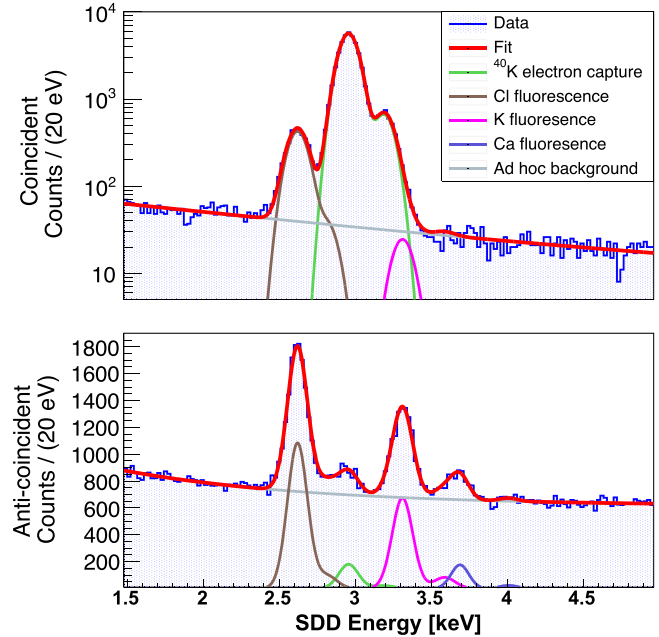

FIG. 2. SDD coincidence and anticoincidence spectra. Results of simultaneous fit to coincident (top) and anticoincident (bottom) SDD spectra at a 2 μs coincidence window. Signal counts are shown in green. Various fluorescence peaks and an exponential background model are included. The total minimization has an associated goodness of fit of $p = 0.4$.

possibly in coincidence with MTAS background. Because of shielding from MTAS, the natural background rate in the SDD is extremely suppressed. The β^+ branch of ^{40}K is also a negligible background. Particulars of the background Cl, K and Ca X-ray fluorescence lines are discussed in Sec. IIA of [27].

Using the spectral elements discussed, a joint likelihood function was developed to describe the coincident and anticoincident binned spectra. It was then minimized to provide an estimator of the ratio of intensities (ρ), a confidence interval, and goodness of fit. An example of a full fit with details of the components is shown in Fig. 2, with details of the anticoincident signal region in Fig. 3. The overall result we obtain is

$$\rho = I_{EC^0}/I_{EC^*} = 0.0095 \overset{\text{stat}}{\pm} 0.0022 \overset{\text{sys}}{\pm} 0.0010.$$

All uncertainties in this Letter correspond to a 68% level confidence interval. This result is consistent over the various coincidence windows, and corresponds to about 500 observed EC^0 events.

As part of the estimation of systematic errors, the fit was repeated for various binnings and histogram ranges. Other contributions to the systematics include uncertainties on physical parameters, the most important of which is the uncertainty on the tagging efficiency, and uncertainties on
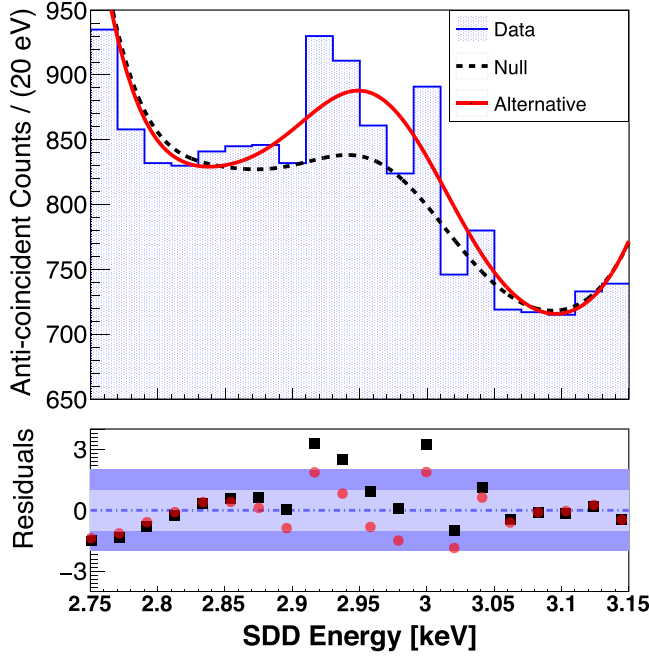
FIG. 3. The anticoincident x-ray signal region corresponding to Fig. 2, showing a fit assuming a null hypothesis of $\rho = 0$ (dashed black) and an alternate fit with ρ free (solid red), returning $\rho = I_{EC^0}/I_{EC^*} = 0.0095 \overset{\text{stat}}{\pm} 0.0022 \overset{\text{sys}}{\pm} 0.0010$. A likelihood ratio test between the two hypotheses returns $p = 2 \times 10^{-5}$ which is equivalent to a 4σ significance. For each bin count o and associated fit value e the residual is defined as $(o-e)/\sqrt{e}$.

the shape of the background continuum. Details are provided in Sec. IID of [27].

We have also performed a likelihood ratio test comparing the null hypothesis ($\rho = 0$, no ground state decay) to the alternative hypothesis (ρ is free). Results are shown in Fig. 3 for the anti-coincident signal region. If the null hypothesis was true, the probability of obtaining a canonical test statistic as large as the one obtained from the data is $p = 2 \times 10^{-5}$. The significance is equivalent to the probability that a Gaussian fluctuation will be at least 4σ above its mean. Our results in terms of central value of ρ and of significance are stable to changes in fitting procedures and models, including those that affect the goodness of fit. This first attempt to measure the elusive ^{40}K electron-capture decay to ground state yields compelling evidence for its existence.

Following the formulation discussed elsewhere (Sec. IIIA of [27]), we reevaluate the decay scheme of ^{40}K [Fig. 1(a)] using the novel ρ parameter and the most recent data evaluations of the partial decay constants of the β^- and EC* branches ($\lambda^- = 0.4904 \pm 0.0019$ Ga^{-1} and $\lambda^* = 0.05646 \pm 0.00016$ Ga^{-1}, Sec. 5.2 of [23]). Our measurement yields a ground-state decay electron-capture branching ratio of $I_{EC^0} = 0.098\% \overset{\text{stat}}{\pm} 0.023\% \overset{\text{sys}}{\pm} 0.010\%$, which is about 50% smaller and 5 times more precise than the value obtained using the generally accepted

comparative half-life ($\log ft$) prediction [21]. This ground state branching ratio is robust within uncertainties for various commonly used sets of decay constants [13,23,32]. Depending on whether experimental or theoretical inputs are added, the branching ratio for β^+ can vary by a factor 2, but remains small and does not affect the rest of the decay scheme within uncertainties.

Our measured EC^0 branching ratio is approximately a factor of 2 smaller than theoretical predictions [8,15,19–22], with the exception of our calculation (Fig. 6 and Sec. IIIB of [27]), 0.058(22)%. As our Letter represents the first measurement of a third-forbidden unique electron-capture, the variance may indicate that fine-tuning is needed in theoretical modeling. This fine-tuning impacts the traditional modelling of nuclear matrix elements of the neutrinoless double-β decay since the present theoretical analyses of the three ^{40}K decay branches, β^-, EC*, and EC^0, imply that the contributions of forbidden transitions to these matrix elements are heavily suppressed. This increases the computed neutrinoless double-beta decay half-life of ^{48}Ca by an estimated factor of 7^{+3}_{-2}, as discussed in Sec. IIIB of [27], adding to the challenge of detecting this rare decay mode.

Moreover, unlike the other theoretical approaches, the calculation of this Letter does not depend on predicting the I_{EC^0}/I_{β^+} ratio and is therefore not reliant on the few, difficult, measurements of the I_{β^+}/I_{β^-} ratio [19,33–37]. Our Letter, combined with theoretical input $I_{EC^0}/I_{\beta^+} = 215.0(31)$ [17], implies $I_{\beta^+}/I_{\beta^-} = (4.9 \pm 1.2) \times 10^{-6}$, less than half the commonly used value [19].

From the standpoint of rare-event searches, our novel measurement enables quantification of the irreducible ^{40}K background in signal regions that cannot be tagged by the 1.46 MeV γ ray. In particular, experiments using NaI are going to great lengths to deal with the low-energy emissions from electron capture; measures include extreme purification of crystals [5,6], veto systems [4,5], and cryogenic particle identification [3]. In addition, the EC^0 decay of ^{40}K may affect the long-standing, but controversial, claim for dark-matter discovery by the DAMA experiment [8]. This argument relies not only on I_{EC^0}, but also on detailed assumptions regarding shapes and intensities of other backgrounds in DAMA [17], and the 1.46 MeV tagging efficiency of that experiment. Our measurement is roughly half the value assumed in [8], tending to relax this type of constraint on the dark-matter interpretation of DAMA.

In geochronology, precision in age-determination has reached $\lesssim 1\%$ [38,39]. Figure 4(a) displays the effect of including the KDK measurement of EC^0 with commonly-used decay constants [13], which reduces K/Ar ages by about 1%. Shown also is the effect of fully updating the decay scheme by combining this Letter with recently reevaluated lifetimes for other ^{40}K transitions [23], which points to underestimation of ages by up to twenty million years. The inclusion of EC^0 has a less dramatic *direct* effect
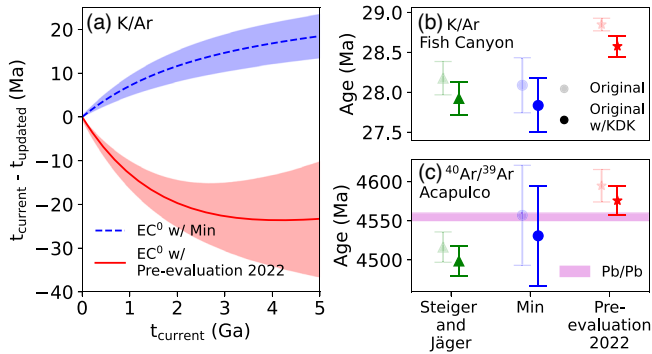
FIG. 4. Effect of updates to ^{40}K decay scheme on geochronology. (a) Variation in K/Ar age when adding the EC^0 branch to commonly used reference decay constants [13] (Min, blue, dashed, errors from EC^0 only) and to the β^- and EC^* branches of a recent literature evaluation (Sec. 5.2 of [23], Kossert preevaluation, red, solid, all errors). In all cases $t_{current}$ represents time calculated using Min decay constants neglecting EC^0. (b) Systematic change in K/Ar age of the Fish Canyon sanidine reference material when EC^0 is added to the previous decay constants and to those in [44]. (c) Updated $^{40}Ar/^{39}Ar$ age of the Acapulco meteorite using the decay constants and reference ages shown in (b). Pb/Pb age is updated from [42]. All uncertainties correspond to a 68% confidence level.

on $^{40}Ar/^{39}Ar$ ages, inducing a variation of about 0.1%, and updating the full decay scheme leads to no change within error. However, there is an *indirect* effect on $^{40}Ar/^{39}Ar$ ages calibrated with K/Ar-dated standards, such as the widely used Fish Canyon sanidine reference material [40], as seen in Figs. 4(b) and 4(c). For instance, Fig. 4(c) reevaluates the age of the Acapulco meteorite [41], one of the oldest known objects in the solar system. The ages derived from the more recent decay constants [13,23] are statistically consistent with ages obtained using the Pb/Pb [42] and Sm/Nd [43] techniques. The variability in the other partial decay branches is now the limiting factor in the ^{40}K decay scheme, which remains a significant source of uncertainty in $^{40}Ar/^{39}Ar$ dating.

We have presented strong evidence for the previously questioned electron-capture decay to the ground state of ^{40}K. This represents the first measured third-forbidden unique electron-capture decay, and will thus be of crucial importance for testing theoretical predictions regarding the high-multipole matrix elements relevant for neutrinoless double-β decay. Our Letter provides a better understanding of low-energy backgrounds in rare-event searches in non-accelerator particle physics. From the standpoint of geochronology, this first measurement of EC^0 as an additional production channel changes the determined age at the order of the current analytical precision for both K/Ar and $^{40}Ar/^{39}Ar$ methods. Our novel measurement revealing an extremely rare decay of a ubiquitous isotope has vast implications in a variety of fields.

---

[*]distefan@queensu.ca
[†]yavin.itay@gmail.com

[1] H. Ejiri, J. Suhonen, and K. Zuber, Neutrino–nuclear responses for astro-neutrinos, single beta decays and double beta decays, Phys. Rep. **797**, 1 (2019).
[2] M. Schumann, Direct detection of WIMP dark matter: Concepts and status, J. Phys. G **46**, 103003 (2019).
[3] G. Angloher *et al.* (COSINUS Collaboration), Simulation-based design study for the passive shielding of the COSINUS dark matter experiment, Eur. Phys. J. C **82**, 248 (2022).
[4] P. Adhikari *et al.* (COSINE-100 Collaboration), Background model for the NaI (Tl) crystals in COSINE-100, Eur. Phys. J. C **78**, 490 (2018).
[5] M. Antonello *et al.* (SABRE Collaboration), Monte Carlo simulation of the SABRE PoP background, Astropart. Phys. **106**, 1 (2019).
[6] J. Amaré *et al.* (ANAIS-112 Collaboration), Annual modulation results from three-year exposure of ANAIS-112, Phys. Rev. D **103**, 102005 (2021).

[7] R. Bernabei et al. (DAMA/LIBRA Collaboration), First model independent results from DAMA/LIBRA–Phase2, Universe **4**, 116 (2018).

[8] J. Pradler, B. Singh, and I. Yavin, On an unverified nuclear decay and its role in the DAMA experiment, Phys. Lett. B **720**, 399 (2013).

[9] G. J. Wasserburg and R. J. Hayden, A^{40}-K^{40} dating, Geochim. Cosmochim. Acta **7**, 51 (1955).

[10] C. Merrihue and G. Turner, Potassium-argon dating by activation with fast neutrons, J. Geophys. Res. **71**, 2852 (1966).

[11] Th. F. Nägler and I. M. Villa, In pursuit of the ^{40}K branching ratios: K-Ca and $^{39}Ar - {}^{40}Ar$ dating of gem silicates, Chem. Geol. **169**, 5 (2000).

[12] F. Begemann, K. R. Ludwig, G. W. Lugmair, K. Min, L. E. Nyquist, P. J. Patchett, P. R. Renne, C.-Y. Shih, I. M. Villa, and R. J. Walker, Call for an improved set of decay constants for geochronological use, Geochim. Cosmochim. Acta **65**, 111 (2001).

[13] K. Min, R. Mundil, P. R. Renne, and K. R. Ludwig, A test for systematic errors in $^{40}Ar/^{39}Ar$ geochronology through comparison with U/Pb analysis of a 1.1-Ga rhyolite, Geochim. Cosmochim. Acta **64**, 73 (2000).

[14] P. R. Renne, R. Mundil, G. Balco, K. Min, and K. R. Ludwig, Joint determination of ^{40}K decay constants and $^{40}Ar*/^{40}K$ for the Fish Canyon sanidine standard, and improved accuracy for $^{40}Ar/^{39}Ar$ geochronology, Geochim. Cosmochim. Acta **74**, 5349 (2010).

[15] J. Carter, R. B. Ickert, D. F. Mark, M. M. Tremblay, A. J. Cresswell, and D. C. W. Sanderson, Production of ^{40}Ar by an overlooked mode of ^{40}K decay with implications for K-Ar geochronology, Geochronology **2**, 355 (2020).

[16] B. Singh, J. L. Rodriguez, S. S. M. Wong, and J. K. Tuli, Review of $\log ft$ values in β decay, Nucl. Data Sheets **84**, 487 (1998).

[17] X. Mougeot, Improved calculations of electron capture transitions for decay data and radionuclide metrology, Appl. Radiat. Isot. **134**, 225 (2018).

[18] X. Mougeot, Towards high-precision calculation of electron capture decays, Appl. Radiat. Isot. **154**, 108884 (2019).

[19] D. W. Engelkemeir, K. F. Flynn, and L. E. Glendenin, Positron emission in the decay of K^{40}, Phys. Rev. **126**, 1818 (1962).

[20] N. B. Gove and M. J. Martin, log-f tables for beta decay, At. Data Nucl. Data Tables **10**, 205 (1971).

[21] LOGFT (accessed August 28th, 2020), with original code from Gove and Martin 1971. available at: https://www.nndc.bnl.gov/logft/.

[22] J. Chen, Nuclear data sheets for A = 40, Nucl. Data Sheets **140**, 1 (2017).

[23] K. Kossert, Y. Amelin, D. Arnold, R. Merle, X. Mougeot, M. Schmiedel, and D. Zapata-García, Activity standardization of two enriched ^{40}K solutions for the determination of decay scheme parameters and the half-life, Appl. Radiat. Isot. **188**, 110362 (2022).

[24] M. Wang, W. J. Huang, F. G. Kondev, G. Audi, and S. Naimi, The AME 2020 atomic mass evaluation (II). Tables, graphs and references, Chin. Phys. C **45**, 030003 (2021).

[25] P. C. F. Di Stefano et al. (KDK Collaboration), The KDK (potassium decay) experiment, J. Phys. Conf. Ser. **1342**, 012062 (2020).

[26] M. Stukel et al. (KDK collaboration), A novel experimental system for the KDK measurement of the ^{40}K decay scheme relevant for rare event searches, Nucl. Instrum. Methods Phys. Res., Sect. A **1012**, 165593 (2021).

[27] L. Hariasz et al., companion paper, Evidence for ground-state electron capture of ^{40}K, Phys. Rev. C **108**, 014327 (2023).

[28] P. Lechner et al., Silicon drift detectors for high resolution room temperature x-ray spectroscopy, Nucl. Instrum. Methods Phys. Res., Sect. A **377**, 346 (1996).

[29] M. Karny, K. P. Rykaczewski, A. Fijałkowska, B. C. Rasco, M. Wolińska-Cichocka, R. K. Grzywacz, K. C. Goetz, D. Miller, and E. F. Zganjar, Modular total absorption spectrometer, Nucl. Instrum. Methods Phys. Res., Sect. A **836**, 83 (2016).

[30] B. Hoeling, D. Reed, and P. B. Siegel, Going bananas in the radiation laboratory, Am. J. Phys. **67**, 440 (1999).

[31] X. Mougeot, BetaShape: A new code for improved analytical calculations of beta spectra, EPJ Web Conf. **146**, 12015 (2017).

[32] M. M. Bé et al., Table of radionuclides (Vol. 5–A = 22 to 244) (2010), https://hal-cea.archives-ouvertes.fr/cea-02476352v1.

[33] P. R. Bell and J. M. Cassidy, Gamma-rays of K^{40}, Phys. Rev. **77**, 409 (1950).

[34] P. R. Bell and J. M. Cassidy, Measurement of the gamma-ray energy of K^{40}, Phys. Rev. **79**, 173 (1950).

[35] S. A. Colgate, The positron activity of K^{40}, Phys. Rev. **81**, 1063 (1951).

[36] D. R. Tilley and L. Madansky, Search for positron emission in K^{40}, Phys. Rev. **116**, 413 (1959).

[37] H. Leutz, G. Schulz, and H. Wenninger, The decay of potassium-40, Z. Phys. **187**, 151 (1965).

[38] E. M. Niespolo, D. Rutte, A. L. Deino, and P. R. Renne, Intercalibration and age of the Alder Creek sanidine $^{40}Ar/^{39}Ar$ standard, Quat. Geochronol. **39**, 205 (2017).

[39] I. McDougall and P. Wellman, Calibration of GA1550 biotite standard for K/Ar and $^{40}Ar/^{39}Ar$ dating, Chem. Geol. **280**, 19 (2011).

[40] K. F. Kuiper, A. Deino, F. J. Hilgen, W. Krijgsman, P. R. Renne, and J. R. Wijbrans, Synchronizing rock clocks of earth history, Science **320**, 500 (2008).

[41] P. R. Renne, $^{40}Ar/^{39}Ar$ age of plagioclase from Acapulco meteorite and the problem of systematic errors in cosmochronology, Earth Planet. Sci. Lett. **175**, 13 (2000).

[42] C. Göpel and G. Manhès, The thermal history of the Acapulco meteorite and its parent body deduced from U/Pb systematics in mineral separates and bulk rock fragments, C. R. Geoscience **342**, 53 (2010).

[43] A. Prinzhofer, D. A. Papanastassiou, and G. J. Wasserburg, Samarium-neodymium evolution of meteorites, Geochim. Cosmochim. Acta **56**, 797 (1992).

[44] R. H. Steiger and E. Jäger, Subcommission on geochronology: Convention on the use of decay constants in geo- and cosmochronology, Earth Planet. Sci. Lett. **36**, 359 (1977).

[45] http://energy.gov/downloads/doe-public-access-plan.